Copy 6
RM A55K21

NACA RM A55K21

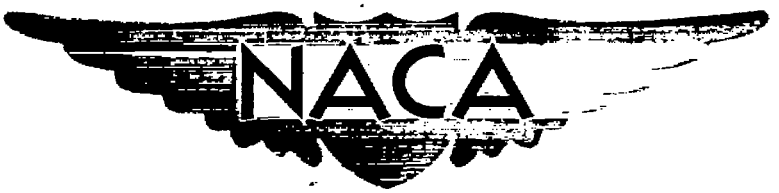

RESEARCH MEMORANDUM

LIFT, DRAG, AND STATIC LONGITUDINAL STABILITY CHARACTERISTICS OF CONFIGURATIONS CONSISTING OF THREE TRIANGULAR WING PANELS AND A BODY OF EQUAL LENGTH AT MACH NUMBERS FROM 3.00 TO 6.28

By Raymond C. Savin and Thomas J. Wong

Ames Aeronautical Laboratory
Moffett Field, Calif.

NATIONAL ADVISORY COMMITTEE
FOR AERONAUTICS

WASHINGTON
February 7, 1956

NACA RM A55K21

NATIONAL ADVISORY COMMITTEE FOR AERONAUTICS

RESEARCH MEMORANDUM

LIFT, DRAG, AND STATIC LONGITUDINAL STABILITY CHARACTERISTICS OF CONFIGURATIONS CONSISTING OF THREE TRIANGULAR WING PANELS AND A BODY OF EQUAL LENGTH AT MACH NUMBERS FROM 3.00 TO 6.28

By Raymond C. Savin and Thomas J. Wong

SUMMARY

Lift, drag, and pitching-moment coefficients, lift-drag ratios, and center-of-pressure positions for three highly swept three-wing tailless configurations were determined from tests at Mach numbers from 3.00 to 6.28 and angles of attack up to 12°. The Reynolds number based on body length varied from 5.5 million at Mach number 3.00 to 1.0 million at Mach number 6.28. Each configuration had three identical triangular-wing panels of low aspect ratio with 2-percent-thick root sections. The leading edges of the panels were rounded and had a constant radius equal to the radius of the vertex of the configuration. One of the wing panels was mounted vertically on the top of the body as a fin. The other two were mounted as the main lifting surfaces. Three separate configurations were obtained by mounting the two lifting wings at dihedral angles of 0°, ±15°, and -30°. The leading edges of the wings were swept back 74°. The body of each configuration consisted of a fineness-ratio-5 ogive and a fineness-ratio-2 cylindrical afterbody. The tip of the ogive was spherical and had a radius equal to 5 percent of the maximum body radius.

The maximum lift-drag ratios decreased slightly with increasing negative dihedral angle throughout the test Mach number range. A maximum lift-drag ratio of 4.5 was obtained for the model with 0° dihedral at a Mach number of 4.26. The static longitudinal stability remained approximately constant with increasing negative dihedral angle, but decreased slightly with increasing Mach number.

INTRODUCTION

A configuration has recently been proposed in reference 1 as an example of an airplane suitable for flight at high supersonic speeds. The proposed airplane configuration was chosen mainly on the basis of

theoretical calculations relating to drag, lift-drag ratio, aerodynamic stability, and aerodynamic heating. Thus, for example, it was indicated that the use of extreme sweepback greatly relieves the heating of the wing leading edge, and, of course, reduces the drag due to leading-edge bluntness. A symmetrical arrangement of three wings, the vertices of which are common to the vertex of the body, was selected on the basis of the more satisfactory stability to be expected from this type of configuration over more conventional airframes. Results of tests on such a configuration (see refs. 2 and 3) indicated that satisfactory aerodynamic stability can in fact be obtained, at least at subsonic speeds.

To determine the high-speed aerodynamic characteristics of an airplane configuration incorporating the features suggested in reference 1, a highly swept symmetrical three-wing tailless model was tested in the Ames 10- by 14-inch supersonic wind tunnel at Mach numbers from 3.00 to 6.28 and angles of attack up to 12°. Two other similar models with wing dihedral angles of 0° and -15° were also tested. The results of these tests are the subject of the present paper.

NOTATION

C_D drag coefficient, $\frac{D}{qS}$

C_L lift coefficient, $\frac{L}{qS}$

C_m pitching-moment coefficient (moment reference: 37 percent of $\bar{c}$), $\frac{m}{qS\bar{c}}$

C_N normal-force coefficient, $\frac{\text{normal force}}{qS}$

$\bar{c}$ mean aerodynamic chord of wing, including portion of wing submerged in body

D drag

L lift

M free-stream Mach number

m pitching moment

q free-stream dynamic pressure

Re Reynolds number based on model length

[redacted]

S area of two panels, including area submerged in body

x_{cp} center-of-pressure location, percent body length from nose

α angle of attack

β $\sqrt{M^2 - 1}$

Γ dihedral angle, measured from the horizontal

APPARATUS AND TESTS

The tests were conducted in the Ames 10- by 14-inch supersonic wind tunnel. A detailed description of the wind tunnel and auxiliary equipment may be found in reference 4. Aerodynamic forces and moments acting on the models were measured by means of a three-component strain-gage balance. Angles of attack up to 4° were obtained by pitching the model-support system. Bent-sting model supports were employed to obtain angles of attack greater than 4°. Axial forces acting on the body base, as determined by the difference between measured base pressures and free-stream static pressures, were subtracted from measured total forces. As a result, the data presented do not include the effects of body-base pressure.

The test models were constructed of steel and consisted of three identical triangular-shaped panels mounted on a body consisting of a fineness-ratio-5 ogive and a fineness-ratio-2 cylindrical afterbody. The tip of the ogive was spherical and had a radius equal to 5 percent of the maximum body radius. As shown in figure 1, the panels were mounted to form a vertical fin and two lifting surfaces or wings with leading-edge sweep angles of 74° and an aspect ratio of 1.15 ($\Gamma = 0^\circ$). The root sections of the wings were 2 percent thick. The leading edges were rounded and had a radius equal to the radius at the vertex of the body. The airfoil section is defined in figure 1. Three models were constructed and were similar except for the wing dihedral angles. Thus, one model had horizontal wings (0° dihedral) whereas the other two had wings with -15° and -30° dihedral angles.

Lift, drag, and pitching-moment coefficients were determined for all three models at angles of attack to about 12° at Mach numbers of 3.00, 4.26, 5.04, and 6.28.[1] The free-stream Reynolds numbers based on the length of the models were:

[1]Pitching-moment data at $M = 6.28$ were obtained only at angles of attack up to 4°.

[redacted]

Mach number	Reynolds number, million
3.00	5.5
4.26	4.8
5.04	2.3
6.28	1.0

The variation in Mach number in the region of the test section where the models were located did not exceed ±0.02 at Mach numbers from 3.00 to 5.04 and ±0.04 at Mach number 6.28. Deviations in free-stream Reynolds number did not exceed ±30,000 from the values given. Errors in angle of attack due to uncertainties in corrections for stream angle and for deflection of the model-support system were less than ±0.2°.

The precision of the experimental results was affected by inaccuracies in the force measurements obtained by the balance system, as well as uncertainties in the determination of free-stream dynamic pressures and base pressures. The resulting maximum possible errors in the aerodynamic force and moment coefficients are shown in the following table:

Mach number	C_D	C_L	C_m
3.00	±0.001	±0.002	±0.003
4.26	±.001	±.002	±.003
5.04	±.002	±.002	±.003
6.28	±.002	±.003	±.003

It should be noted that the experimental results presented herein are generally in error by less than these estimates.

RESULTS AND DISCUSSION

Results of the tests of the three models are presented in table I, where lift, drag, pitching-moment and normal-force coefficients, lift-drag ratios, and centers of pressure at various angles of attack are tabulated for all the models over the test Mach number range. All of these data are based on the same reference area which is equal to twice the plan area of one panel, including the portion submerged in the body. Graphical presentation of some of the data is also included to show the more important trends. It will be noted in figure 2, for example, that although the differences in lift between the three test models are small, the model with $\Gamma = -15^\circ$ has the highest lift at the higher angles of attack, whereas the symmetrical model ($\Gamma = -30^\circ$) tends to have the lowest lift. These results differ from those obtained at subsonic speeds (ref. 3) where it was found that the lift coefficient decreased approximately as the square of the cosine of the dihedral angle. It should be

noted, however, that the leading edges of the present test models are considerably more blunt than those of reference 3. The effect of leading-edge bluntness on lift at $\alpha = 0^\circ$ is clearly evident in figure 2. Thus, it is observed that although the pressure forces on the blunt leading edges are balanced in the case of the symmetrical model ($\Gamma = -30^\circ$), these forces produce negative lift when the wings are at 0° and -15° dihedral angles. It may also be noted in figure 2, however, that the initial lift-curve slopes do decrease approximately as the square of the cosine of the dihedral angle. This is perhaps more clearly illustrated in figure 3 where the initial slopes taken from figure 2 are shown plotted as a function of Mach number. The predictions of linear airfoil theory for the wing alone ($\Gamma = 0^\circ$) are also shown for comparative purposes in the range of Mach numbers where the leading edges are supersonic. It is interesting to note that the percentage effect of dihedral angle on lift-curve slope is approximately constant with increasing Mach number.

The variations of lift coefficient with drag coefficient, pitching-moment coefficient, and lift-drag ratio for the three models are shown in figure 4. It can be seen that, in general, the model with $\Gamma = -15^\circ$ has the lowest drag for a given lift coefficient (particularly at the higher angles of attack) except near lift coefficients where the maximum lift-drag ratios occur. At these lift coefficients (near $(L/D)_{max}$) the model with 0° dihedral has the lowest drag and, hence, the highest lift-drag ratios. The symmetrical model ($\Gamma = -30^\circ$) has generally the highest drag for a given lift coefficient and, thus, yields the lowest lift-drag ratios.

The variations of pitching-moment coefficient with lift coefficient are nearly the same for all three configurations and are approximately linear over the test range of angles of attack and Mach numbers (see fig. 4). It is also indicated in figure 4 that the static longitudinal stability of each model decreases slightly with increasing Mach number. This trend is more clearly illustrated in figure 5 where it can be seen that the change in stability from Mach number 3.00 to Mach number 6.28 represents a shift in the neutral point of about 1-1/2 percent of the mean aerodynamic chord. Experimental results (see ref. 3) obtained at subsonic speeds for configurations similar to those employed in the present tests are also shown in figure 5. It is indicated that, in general, the neutral points shift rearward on all configurations in going from Mach number 0.25 to Mach number 3.00. This shift is approximately 7 percent of the mean aerodynamic chord in the case of the symmetrical model ($\Gamma = -30^\circ$).

The variations of maximum lift-drag ratio with Mach number are presented in figure 6. It is observed in this figure that the model with 0° dihedral yields the highest lift-drag ratio ($L/D = 4.5$ at $M = 4.26$). However, this ratio decreases only slightly with increasing negative dihedral angle, the total decrease (from $\Gamma = 0^\circ$ to $\Gamma = -30^\circ$) being approximately 5 to 7 percent over the test Mach number range. It should be noted that for Mach numbers 3.00 and 4.26 where the test Reynolds

numbers were essentially the same, the maximum lift-drag ratios are nearly the same. However, at Mach numbers 5.04 and 6.28 where the test Reynolds numbers were substantially lower, the lift-drag ratios are significantly lower. Thus, it is indicated that the decrease in maximum lift-drag ratio with increasing Mach number above $M = 4.26$ is due primarily to the increase in skin-friction drag associated with the decrease of test Reynolds number. The effect of Reynolds number on lift-drag ratio is more clearly shown in figure 7 where estimated lift-drag ratios for a constant Mach number of 5.04 are plotted as a function of Reynolds number.[2] It is indicated in this figure that if the $M = 5.04$ tests were conducted at a Reynolds number of 5 million (i.e., a test Reynolds number approximately the same as that for the lower Mach numbers) instead of 2.3 million, a maximum lift-drag ratio of the same order as those at the lower Mach numbers would have been obtained. Correspondingly, an increase in lift-drag ratio with an increase of test Reynolds number at $M = 6.28$ would also be expected. Moreover, it is indicated that lift-drag ratios of the order of 5 can be expected for full-scale Reynolds numbers (of the order of 15 million), provided laminar flow can be maintained. It may be noted, however, that the estimated lift-drag ratios are somewhat lower than those predicted in reference 1. This can be attributed to the fact that the test configurations had considerably more leading-edge bluntness than the proposed configuration (ref. 1).

CONCLUSIONS

The aerodynamic characteristics of three highly swept three-wing tailless configurations having wing dihedral angles of 0°, -15°, and -30° have been determined from tests at Mach numbers from 3.00 to 6.28 and angles of attack up to 12°. The Reynolds number based on body length varied from 5.5 million at Mach number 3.00 to 1.0 million at Mach number 6.28. The following conclusions are drawn from the results of these tests:

1. The differences in lift between the three test models are small. The initial lift-curve slopes decrease with increasing negative dihedral angle and, as would be expected, also decrease with increasing Mach number.

---

[2]The lift-drag ratios shown in figure 7 were estimated by means of the approximate relation $(L/D)_{max} = 1/2\sqrt{(C_{L_\alpha})_{\alpha=0}/C_{D_o}}$. The lift-curve slope, $(C_{L_\alpha})_{\alpha=0}$, was determined from the experimental results for a Mach number of 5.04 (see fig. 3). The effects of varying Reynolds number on C_{D_o} was estimated by means of the Blasius relation for laminar skin-friction coefficient.

2. The 0° dihedral model was found to have a maximum lift-drag ratio of 4.5 at a Mach number of 4.26. Increasing the dihedral angle from 0° to -30° decreases the maximum lift-drag ratio approximately 5 to 7 percent over the test Mach number range. This ratio also decreases with increasing Mach number due primarily to the increased skin-friction drag associated with the decrease of the test Reynolds number.

3. The static longitudinal stability remains approximately constant with increasing negative dihedral angle, but decreases slightly as the Mach number is increased.

Ames Aeronautical Laboratory
National Advisory Committee for Aeronautics
Moffett Field, Calif., Nov. 21, 1955

REFERENCES

1. Seiff, Alvin, and Allen, H. Julian: Some Aspects of the Design of Hypersonic Boost-Glide Aircraft. NACA RM A55E26, 1955.

2. Delany, Noel K.: Exploratory Investigation of the Low-Speed Static Stability of a Configuration Employing Three Identical Triangular Wing Panels and a Body of Equal Length. NACA RM A55C28, 1955.

3. Delany, Noel K.: Additional Measurements of the Low-Speed Static Stability of a Configuration Employing Three Triangular Wing Panels and a Body of Equal Length. NACA RM A55F02a, 1955.

4. Eggers, A. J., Jr., and Nothwang, George J.: The Ames 10- By 14-Inch Supersonic Wind Tunnel. NACA TN 3095, 1954.

[redacted]

TABLE I.- EXPERIMENTAL RESULTS

M	α	C_L	C_D	C_m	C_N	L/D	x_{cp}	M	α	C_L	C_D	C_m	C_N	L/D	x_{cp}
(a) $\Gamma = 0^\circ$ model															
3.00	-4.23	-0.088	0.022	0.010	-0.089	-3.98	65.1	5.04	-4.05	-0.061	0.017	0.005	-0.062	-3.64	63.6
	-2.13	-.050	.017	.007	-.050	-2.96	67.0		-2.03	-.034	.012	.003	-.035	-2.75	63.2
	-1.07	-.029	.015	.004	-.029	-1.95	67.6		-1.02	-.020	.011	.001	-.020	-1.78	62.4
	-.02	-.007	.014	.002	-.008	-.50	69.5		0	-.006	.010	0	-.006	-.60	56.0
	1.04	.014	.014	-.001	.014	1.00	63.7		1.01	.009	.010	-.002	.009	.89	70.3
	2.09	.036	.015	-.004	.036	2.41	65.7		2.02	.024	.011	-.003	.024	2.17	67.5
	4.21	.079	.019	-.010	.080	4.08	66.2		3.03	.037	.012	-.005	.038	3.07	66.7
	6.22	.122	.028	-.014	.125	4.40	65.3		4.04	.066	.016	-.006	.067	4.08	64.7
	8.35	.163	.038	-.019	.167	4.24	65.4		6.46	.086	.021	-.009	.088	4.19	64.4
	10.48	.202	.052	-.022	.208	3.88	65.2		7.98	.108	.026	-.011	.110	4.09	64.3
	12.61	.244	.069	-.028	.253	3.56	65.4		9.98	.137	.036	-.015	.142	3.75	64.7
									12.01	.168	.049	-.016	.175	3.44	63.9
4.26	-2.05	-.038	.013	.005	-.038	-2.99	66.2	6.28	-2.03	-.033	.015	.002	-.033	-2.16	61.6
	-.01	-.006	.011	.002	-.006	-.61	72.8		-1.02	-.020	.014	0	-.020	-1.37	59.4
	2.04	.026	.011	-.003	.027	2.43	64.6		-.01	-.006	.014	0	-.006	-.45	53.7
	2.96	.045	.013	-.003	.046	3.40	63.6		1.01	.008	.014	-.003	.009	.61	76.7
	5.02	.078	.018	-.006	.079	4.40	63.7		2.02	.023	.014	-.004	.023	1.58	68.9
	6.56	.100	.022	-.010	.102	4.50	63.2		3.03	.036	.015	-.005	.037	2.40	67.1
	8.10	.123	.028	-.013	.126	4.35	64.4		4.04	.050	.017	-.006	.051	2.99	66.5
	10.12	.154	.040	-.015	.159	3.88	64.2		4.90	.056	.018	---	.057	3.00	---
	12.18	.186	.053	-.018	.193	3.50	64.3		6.41	.075	.022	---	.076	3.41	---
									7.92	.095	.027	---	.098	3.54	---
									9.90	.123	.037	---	.127	3.33	---
									11.92	.154	.047	---	.160	3.25	---
(b) $\Gamma = -15^\circ$ model															
3.00	-4.21	-0.080	0.022	0.009	-0.081	-3.64	65.1	5.04	-3.03	-0.042	0.013	0.003	-0.043	-3.13	62.8
	-2.11	-.043	.016	.005	-.044	-2.69	65.3		-2.02	-.030	.012	.002	-.031	-2.54	63.3
	-1.06	-.024	.015	.003	-.024	-1.60	65.4		-1.01	-.018	.011	.002	-.018	-1.64	64.8
	-.01	-.005	.014	.001	-.005	-.36	70.3		0	-.003	.010	0	-.003	-.33	56.8
	1.04	.016	.014	-.002	.016	1.14	65.0		1.01	.010	.010	-.001	.010	1.00	66.5
	2.09	.036	.015	-.004	.037	2.40	65.5		2.02	.024	.011	-.003	.025	2.26	64.9
	4.20	.079	.020	-.010	.080	3.95	66.1		3.03	.038	.012	-.004	.039	3.11	65.3
	6.23	.125	.028	-.014	.127	4.39	65.5		4.95	.068	.018	-.006	.070	3.87	63.7
	8.36	.168	.039	-.019	.172	4.29	65.5		6.47	.090	.022	-.008	.092	4.04	63.9
	10.50	.211	.054	-.025	.217	3.89	65.7		7.99	.113	.028	-.010	.116	3.97	63.6
	12.64	.254	.072	-.029	.264	3.51	65.4		9.99	.148	.039	-.016	.153	3.72	65.0
									12.02	.183	.053	-.019	.189	3.44	64.8
4.26	-3.07	-.048	.014	.004	-.049	-3.36	63.5	6.28	-2.03	-.029	.016	.001	-.029	-1.77	60.6
	-2.05	-.035	.013	.003	-.035	-2.73	63.3		-1.02	-.017	.015	0	-.017	-1.08	58.6
	-1.03	-.020	.011	.002	-.020	-1.77	63.1		0	-.004	.015	0	-.004	-.28	46.6
	-.01	-.005	.011	.002	-.005	-.45	71.4		1.01	.010	.015	-.002	.010	.65	67.4
	1.02	.011	.011	-.001	.011	1.02	62.4		2.02	.024	.015	-.003	.024	1.53	67.2
	2.04	.026	.011	-.002	.027	2.30	63.8		3.03	.038	.017	-.005	.038	2.26	66.0
	3.06	.042	.013	-.004	.042	3.24	64.3		4.04	.051	.018	-.006	.052	2.84	65.3
	5.02	.078	.018	-.006	.079	4.24	63.0		4.91	.058	.020	---	.060	2.96	---
	6.57	.102	.023	-.008	.104	4.37	63.4		6.42	.079	.024	---	.081	3.30	---
	8.12	.127	.030	-.012	.130	4.26	63.9		7.93	.101	.029	---	.104	3.44	---
	10.14	.164	.042	-.018	.169	3.93	65.1		9.91	.133	.039	---	.138	3.38	---
	12.20	.198	.056	-.022	.206	3.52	65.1		11.92	.166	.052	---	.173	3.22	---
(c) $\Gamma = -30^\circ$ model															
3.00	-4.16	-0.058	0.020	0.002	-0.059	-2.92	60.6	5.04	-3.03	-0.033	0.012	0.002	-0.033	-2.64	62.8
	-2.09	-.033	.016	.003	-.034	-2.08	64.1		-2.02	-.022	.011	.001	-.023	-1.99	61.8
	-1.05	-.018	.015	.002	-.019	-1.25	66.0		-1.01	-.012	.010	.001	-.012	-1.17	64.9
	0	-.002	.014	0	-.002	-.14	74.1		0	-.001	.010	0	-.001	-.10	72.1
	1.04	.015	.014	-.001	.015	1.05	63.7		1.01	.011	.010	-.001	.011	1.10	62.2
	2.09	.034	.016	-.004	.034	2.13	65.0		2.02	.024	.011	-.002	.024	2.15	63.4
	4.18	.071	.019	-.008	.072	3.69	65.4		3.03	.035	.012	-.003	.036	2.87	62.9
	6.19	.114	.027	-.013	.116	4.21	65.5		4.94	.052	.017	-.006	.053	3.68	63.9
	8.34	.153	.038	-.017	.157	4.03	65.5		6.46	.085	.022	-.009	.087	3.92	65.3
	10.48	.194	.052	-.023	.200	3.72	65.6		7.98	.107	.028	-.012	.110	3.85	65.2
	12.62	.235	.070	-.028	.245	3.38	65.6		9.98	.137	.038	-.012	.142	3.62	63.8
									12.01	.170	.051	-.015	.176	3.33	63.7
4.26	-3.05	-.037	.014	.003	-.037	-2.69	63.2	6.28	-2.02	-.023	.015	.001	-.023	-1.51	59.9
	-2.04	-.026	.012	.003	-.027	-2.16	65.0		-1.01	-.013	.014	0	-.013	-.90	60.3
	-1.02	-.015	.011	.002	-.015	-1.31	66.5		0	-.002	.014	0	-.002	-.14	51.3
	0	-.002	.011	.001	-.002	-.17	86.4		1.01	.011	.014	-.002	.011	.76	71.7
	1.02	.012	.011	-.001	.012	1.08	62.2		2.02	.023	.015	-.004	.024	1.57	68.6
	2.04	.025	.012	-.002	.025	2.16	63.7		3.03	.036	.016	-.004	.036	2.27	66.3
	3.06	.039	.013	-.003	.039	3.01	63.5		4.04	.048	.017	-.006	.050	2.80	65.1
	5.01	.071	.018	-.006	.072	3.98	63.6		4.90	.055	.019	---	.057	2.98	---
	6.56	.094	.022	-.007	.096	4.19	63.2		6.41	.074	.023	---	.076	3.28	---
	8.10	.117	.028	-.010	.120	4.14	63.5		7.89	.093	.028	---	.096	3.34	---
	10.12	.153	.040	-.016	.157	3.79	64.8		9.90	.122	.037	---	.127	3.24	---
	12.18	.187	.054	-.020	.194	3.48	64.8		11.92	.154	.050	---	.161	3.09	---

[redacted]

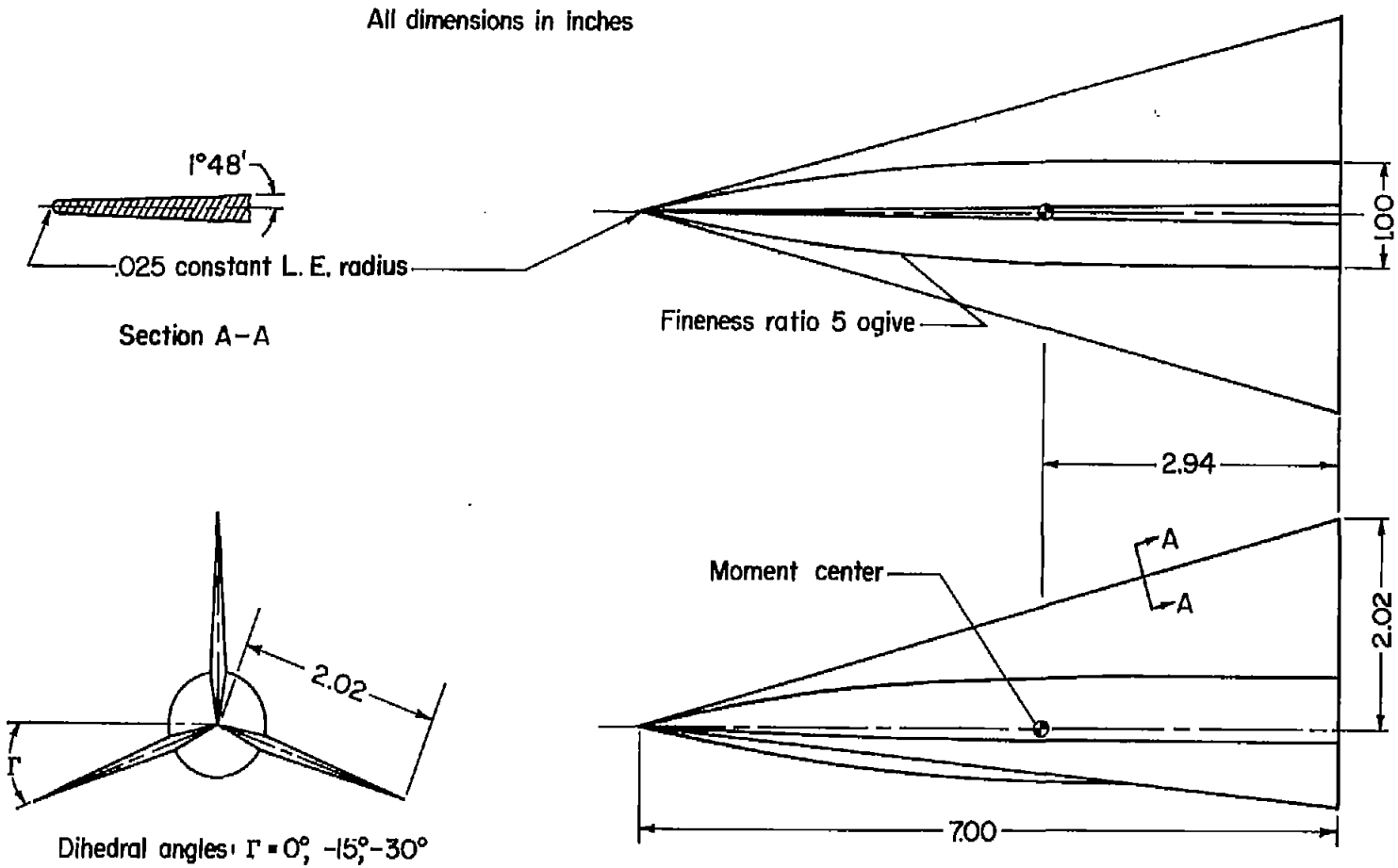

Figure 1.- Details of test models.

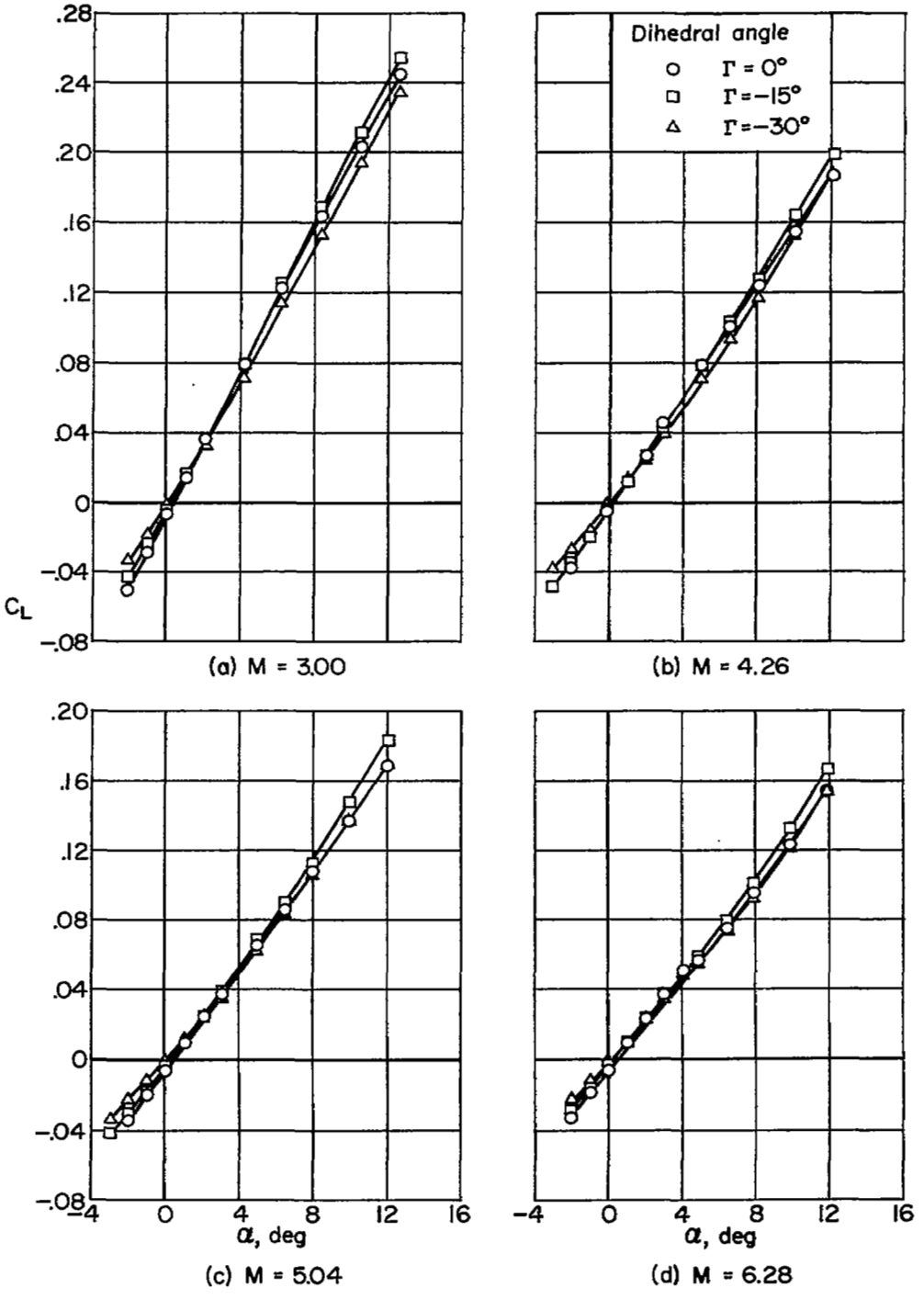

Figure 2.- Variation of lift coefficient with angle of attack.

[redacted]

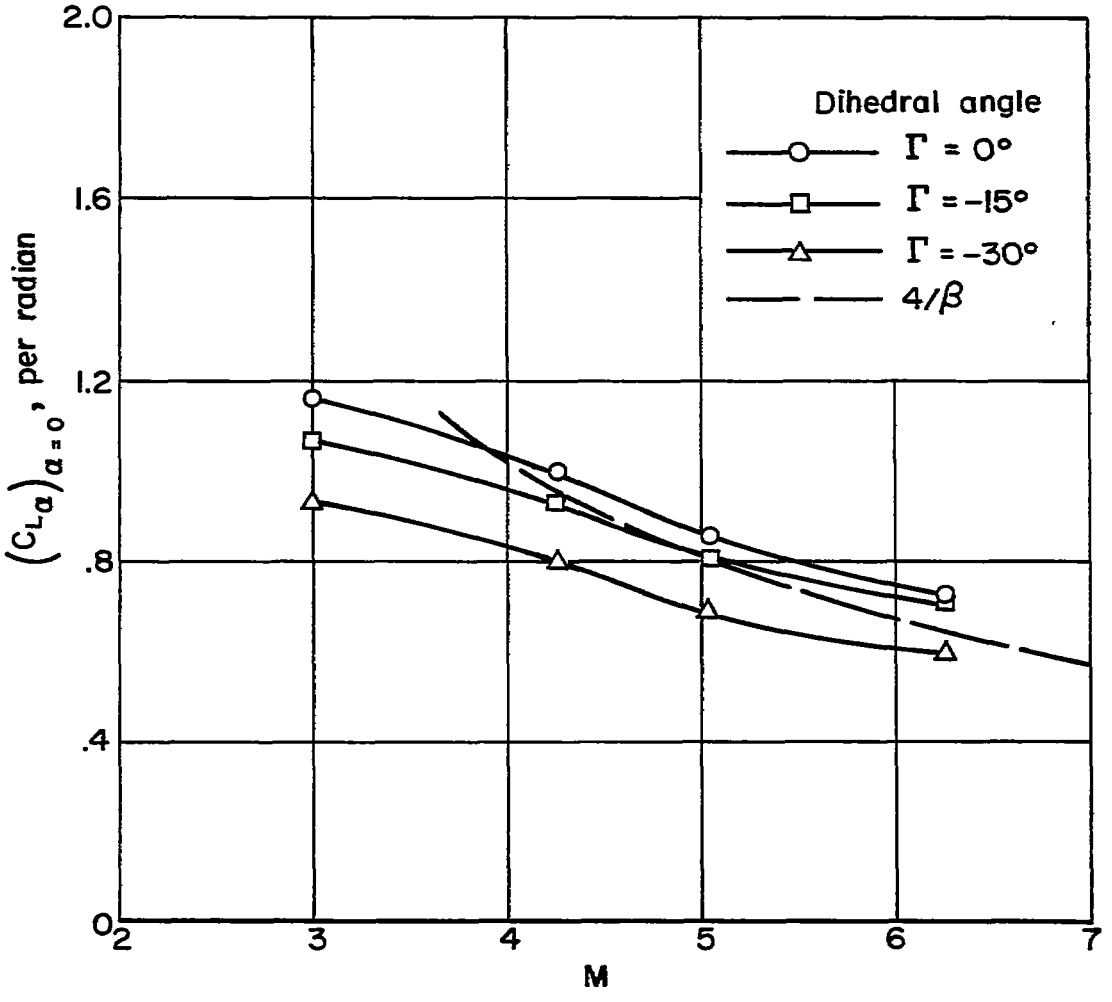

Figure 3.- Variation of initial lift-curve slope with Mach number.

[redacted]

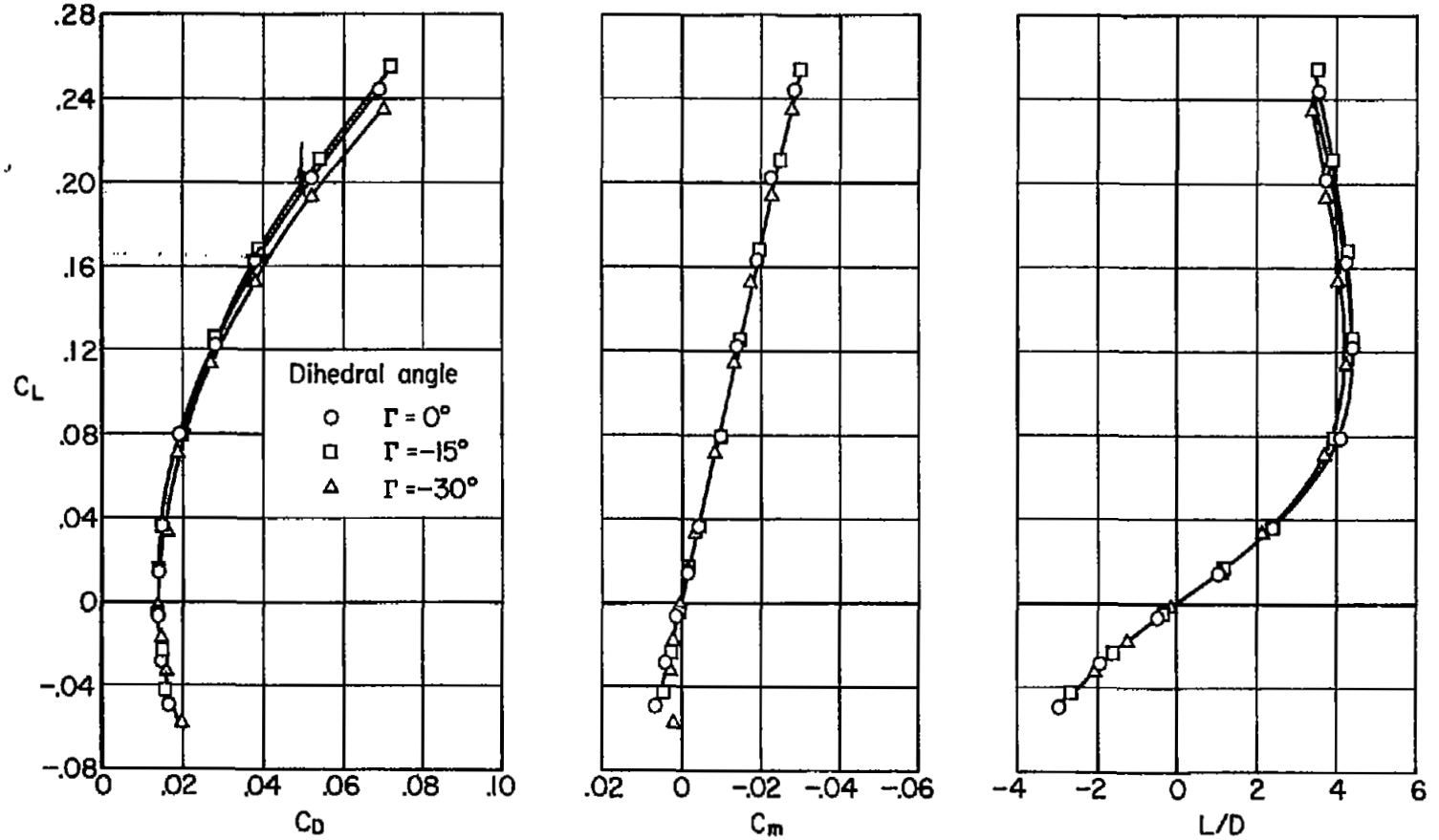

(a) M = 3.00

Figure 4.- Aerodynamic characteristics of test models.

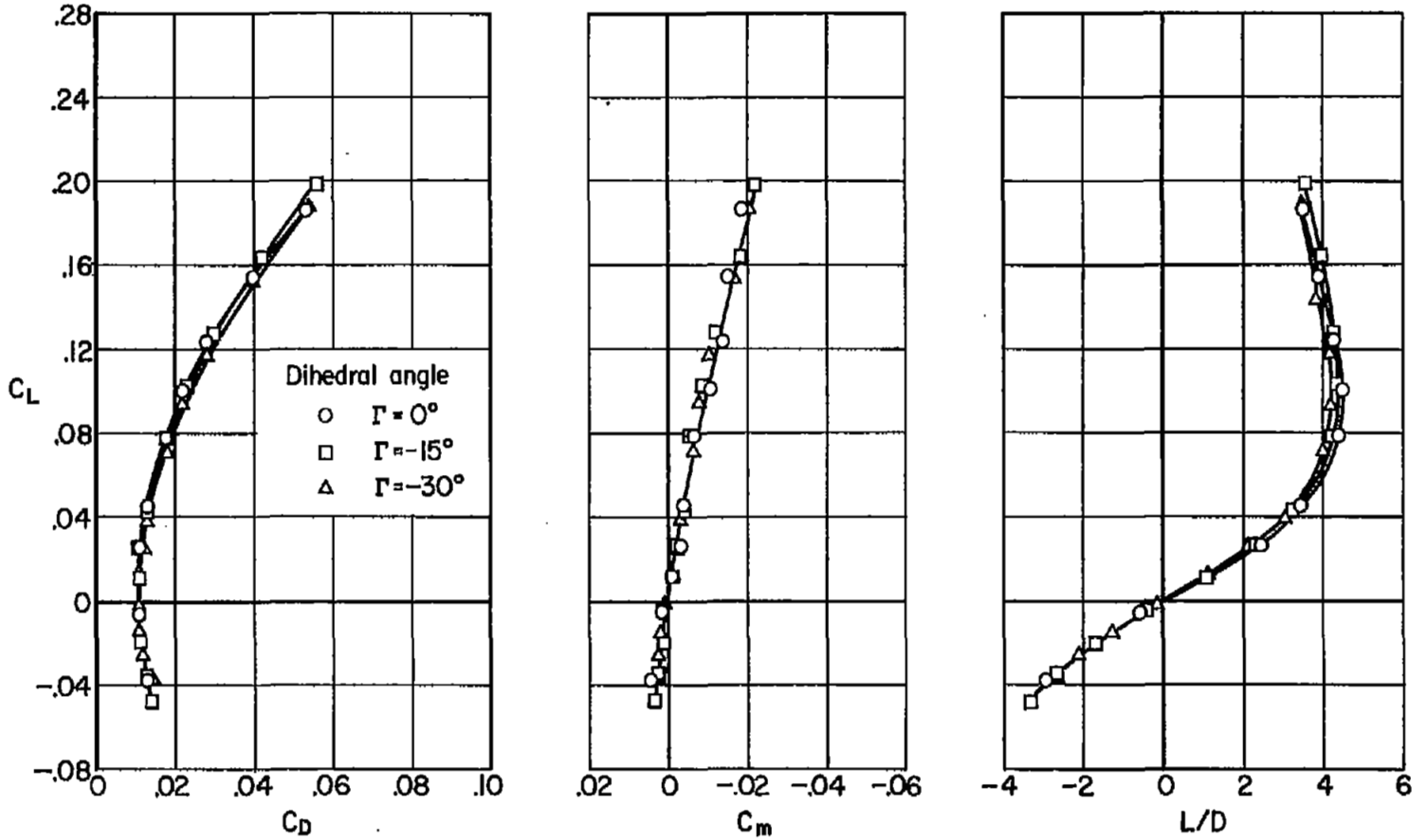

(b) M = 4.26

Figure 4.- Continued.

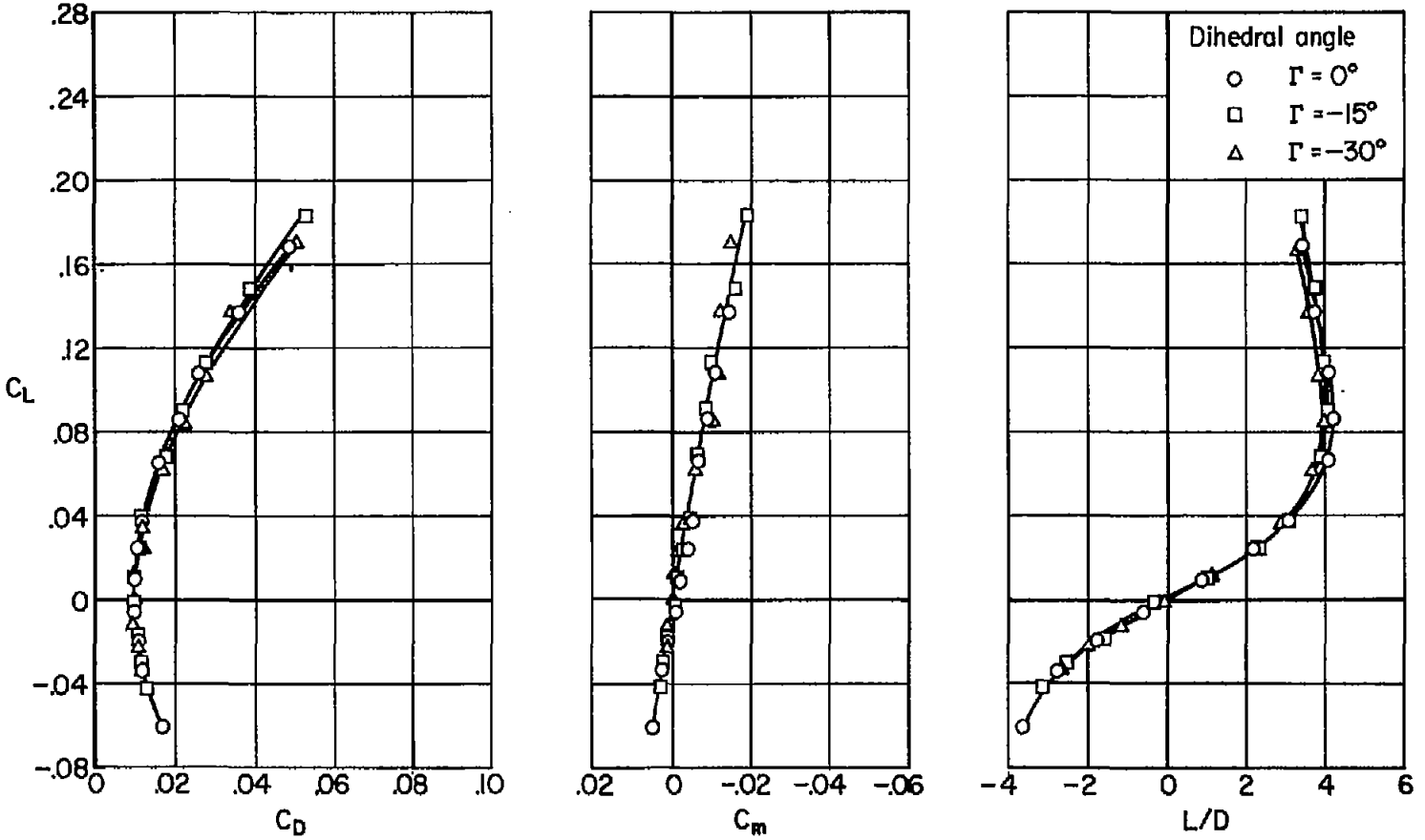

(c) M = 5.04

Figure 4.- Continued.

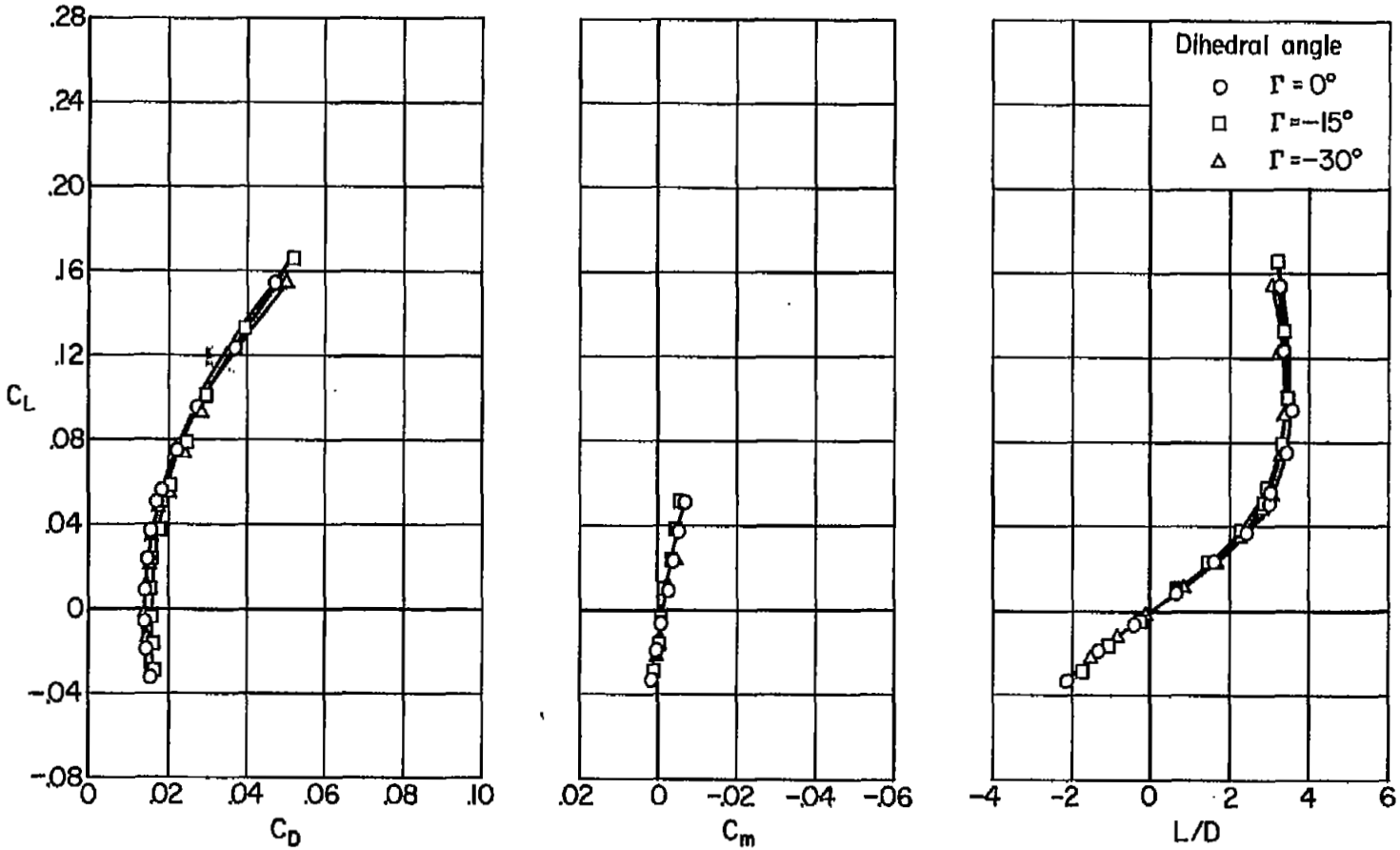

(d) M = 6.28

Figure 4.- Concluded.

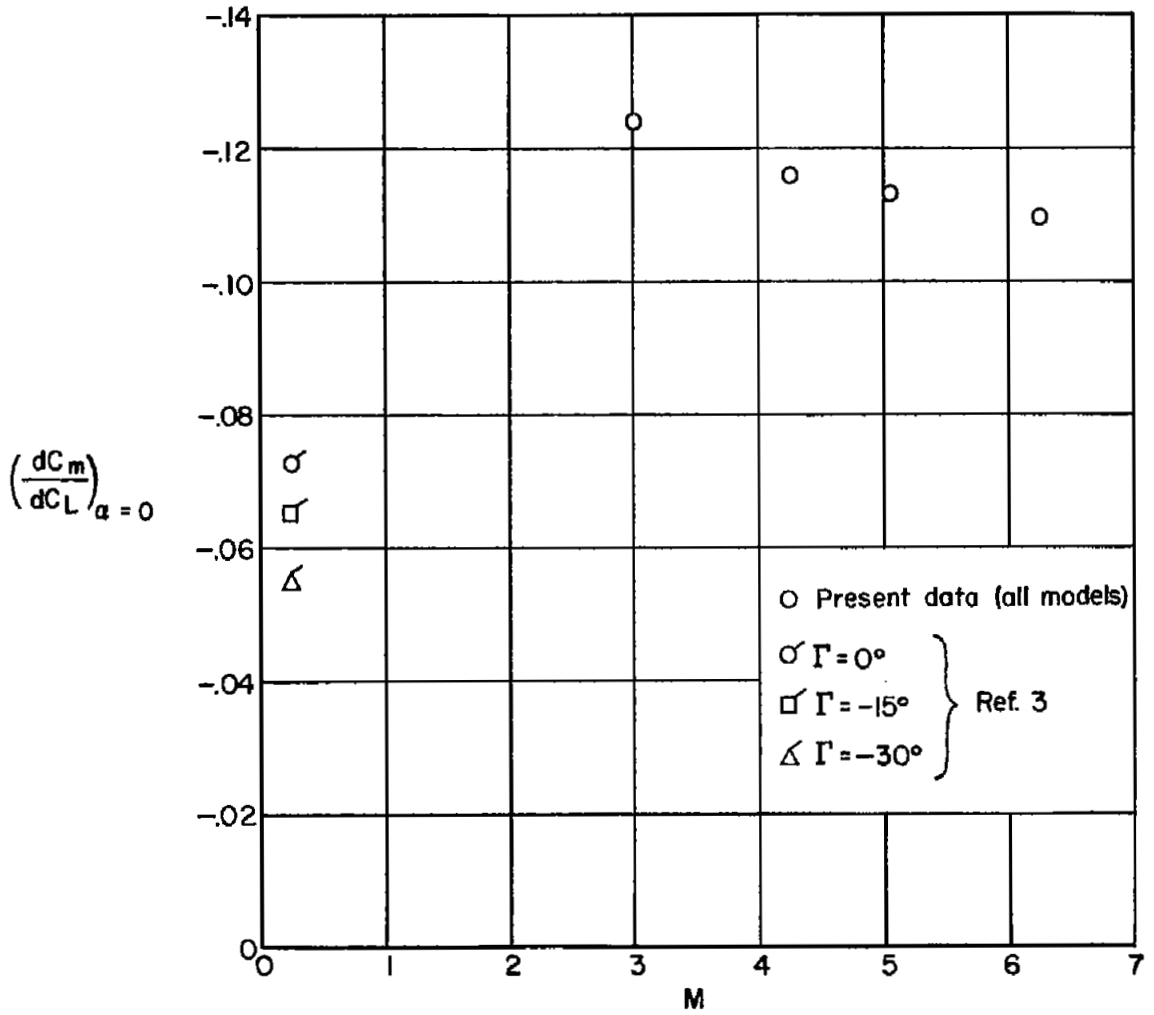

Figure 5.- Variation of static longitudinal stability near zero lift with Mach number (moment reference: 37 percent of $\bar{c}$).

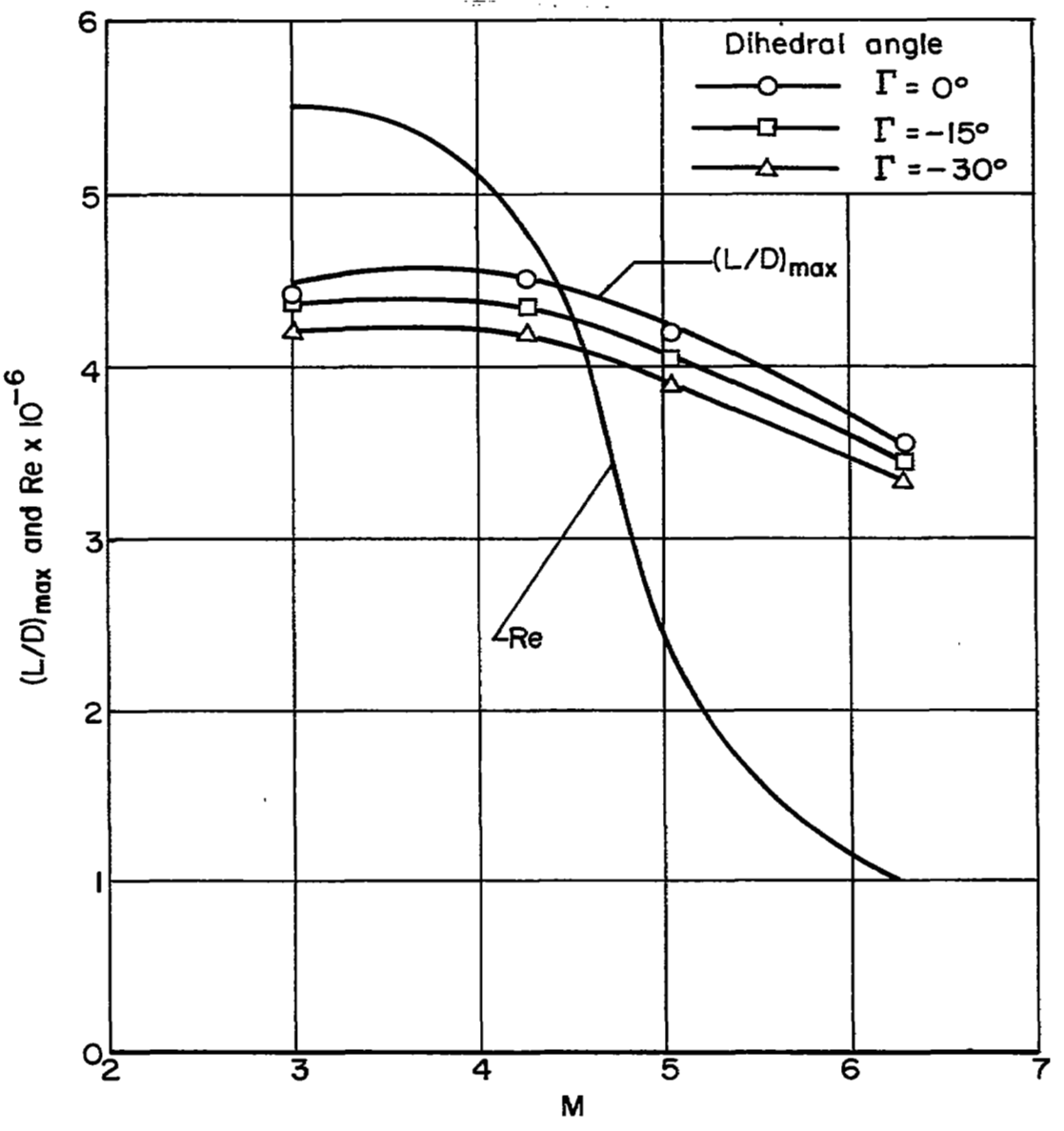

Figure 6.- Variation of maximum lift-drag ratio and Reynolds number with Mach number.

[redacted]

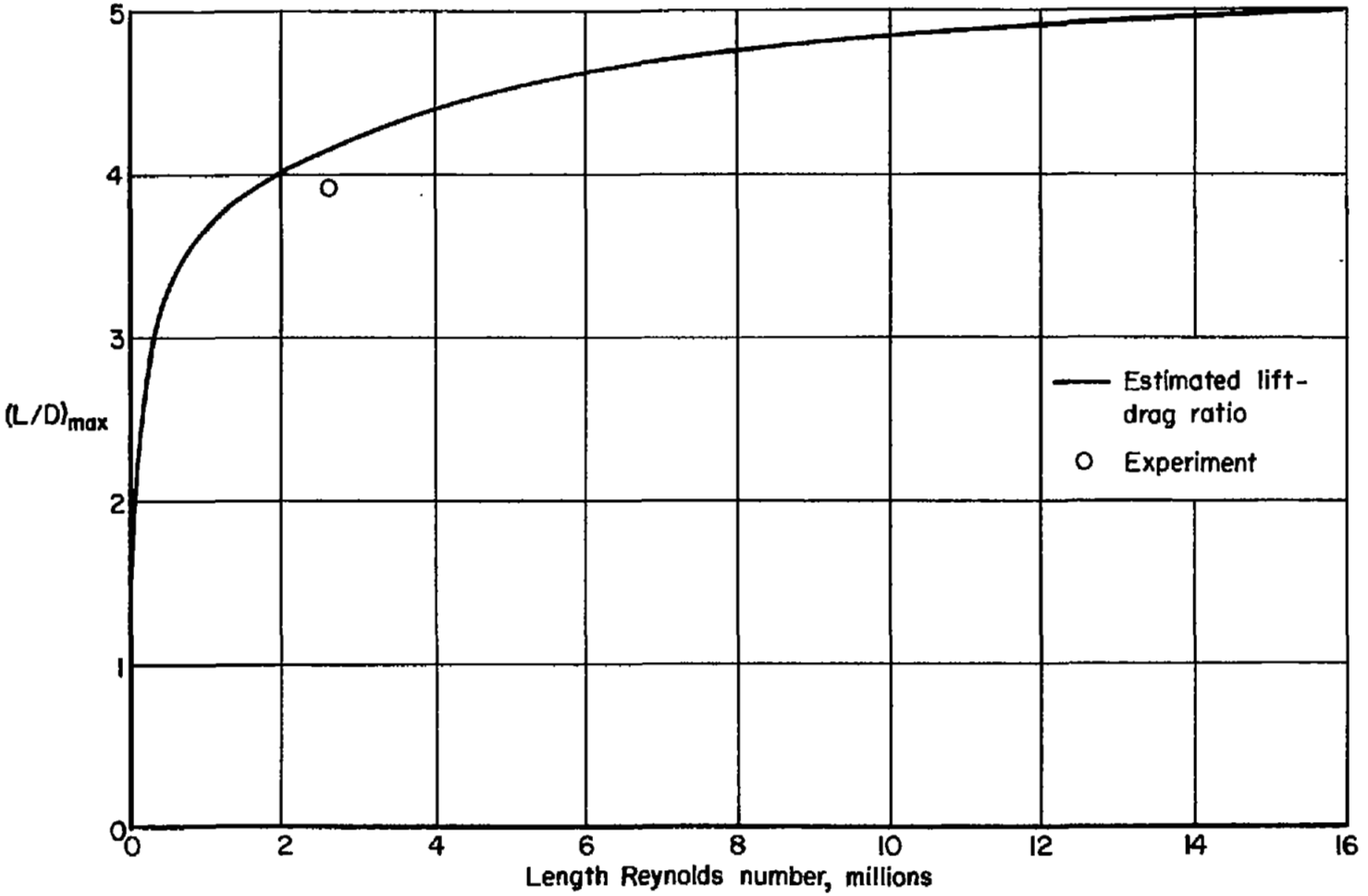

Figure 7.- Variation of maximum lift-drag ratio with Reynolds number for symmetrical configuration ($\Gamma = -30^{\circ}$) at M = 5.04.